Competition between Burgers mechanism and Bain deformation in alkaline-earth metals: Host-guest structures of barium and strontium

Hannelore Katzke[1,*] and Pierre Tolédano[2]

[1]*Crystallography, Institute of Geosciences, University of Kiel, Olshausenstraße 40, 24098 Kiel, Germany*
[2]*Department of Physics, University of Picardie, 33 rue Saint-Leu, 80000 Amiens, France*

The structural mechanisms underlying the high-pressure phase transitions in alkaline-earth metals are described and analyzed theoretically in the framework of an extension of the Landau approach to reconstructive phase transitions. All the high-pressure structures are interpreted as resulting from the full or partial realization of the Burgers and Bain deformation mechanisms. The host-guest structures found in strontium and barium are shown to reflect the competition between the two preceding mechanisms, which expresses at the structural level the competition occurring at the electronic level between the bonding changes induced on pressurization. Further experimental measurements and calculations are suggested for testing our theoretical analysis of the transition mechanisms.

I. INTRODUCTION

The bcc-fcc and bcc-hcp reconstructive phase transitions are the most common structural changes taking place in elemental crystals. Both transitions are found to occur, by varying temperature or pressure, in more than 20 elements belonging to almost all the elemental groups.[1,2] Due to the absence of group-subgroup relationship between the bcc and close-packed hcp and fcc structures, the transitions are described by specific displacive mechanisms going through intermediate stages corresponding to common substructures of the initial (bcc) and final (hcp or fcc) structures. Thus, the bcc-to-hcp Burgers mechanism[3] assumes an intermediate orthorhombic substructure having the *Cmcm* symmetry,[4–6] whereas the bcc-to-fcc Bain deformation mechanism[7] implies going through a tetragonal structure of symmetry $I4/mmm$.[4–6] The influence of Burgers and Bain deformation mechanisms on the polymorphism of the elements goes beyond the simple occurrence of the bcc-hcp and bcc-fcc transitions and can manifest itself by giving rise to structures which reflect either an incomplete realization of one of the two mechanisms or a competition between them. The former situation is attested by the observation of the *Cmcm* intermediate structure assumed for Burgers mechanism in the lanthanide and actinide elements Ce, Pr, Nd, Am, Cm, Bk, and Cf,[8,9] or of the $I4/mmm$ intermediate Bain deformation in Ce, Sm, Pa, and Pu.[8,9] The onset of structures resulting from a competition between the two mechanisms can be illustrated by alkaline-earth metals, which constitute the subject of the present paper.

The high-pressure structures of alkaline-earth metals have been determined up to about 182 GPa for Be,[10] 58 GPa for Mg,[11] 139 GPa for Ca,[12] 75 GPa for Sr,[13] and 90 GPa for Ba,[14] and are summarized in Fig. 1. Therefore, one may attempt to give a unifying description of the mechanisms underlying their structural transitions, going beyond the general theoretical argument of a transfer of electrons from *s-p* to *d* character, which is currently proposed for justifying the polymorphism of the heavier alkaline-earth metals.[15,16] In particular, a number of recent observations still remain to be understood, such as (1) the unusual structural sequence disclosed in strontium above the bcc structure,[13,17,18] which goes from the unexpected β-tin-type structure of Sr III to the host-guest structure of Sr V via the intermediate unique monoclinic structure of Sr IV; (2) the existence of a similar, but different, host-guest structure in barium showing successive guest structures,[19] which separates two hcp structures with different c/a axial ratios;[14] and (3) the highly unexpected stabilization at high pressure of a simple cubic structure in calcium. Here, we show that these observations can be explained by the underlying competition, or alternative domination, of Burgers and Bain mechanisms.

The paper is organized as follows. In Sec. II, we describe the structural mechanisms relating the different structures found under pressure in the alkaline-earth metals in terms of atomic displacements and macroscopic strains. In Sec. III, the preceding description is analyzed and discussed in the framework of the Landau theory of phase transitions, in connection with the influence of the change of electronic structures on the sequences of high-pressure phases. In Sec. IV, we propose a possible explanation for the ubiquitous stabilization of very similar host-guest structures in different groups of elements, and suggest a number of ideas for further verifications of our proposed description.
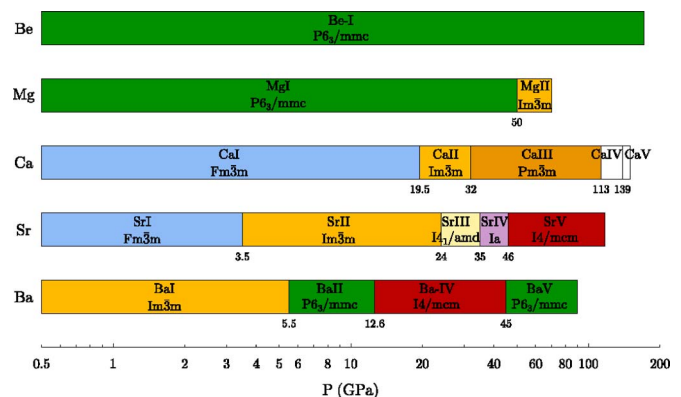
FIG. 1. (Color online) Symmetry of the phases taking place with increasing pressure in the elements of group IIa.
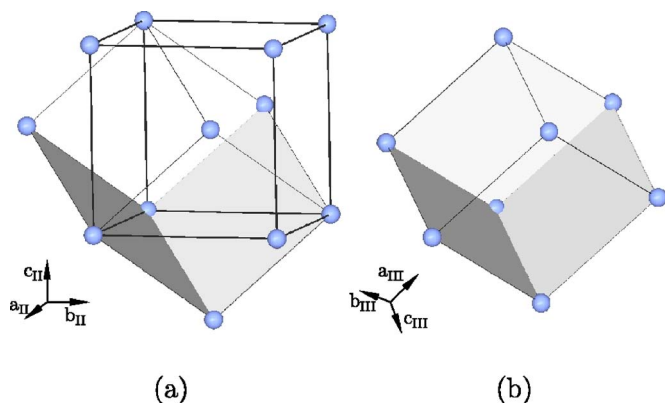
FIG. 2. (Color online) (a) Mechanism of the ferroelastic deformation of the bcc structure of Ca II leading to the simple cubic structure of Ca III shown in (b).

II. STRUCTURAL MECHANISMS IN THE ALKALINE-EARTH METALS

A. Beryllium and magnesium

At room temperature, beryllium has the hcp structure with a c/a ratio of 1.568,[20] which increases up to 1.60 at 180 GPa,[10] far from the ideal value of 1.633. With increasing temperature, the hcp-bcc transition takes place at 1523 K,[21] the transition line having a negative slope of 45 K/GPa up to 6 GPa, which can be assumed to reduce at higher pressures since the bcc phase is not observed at ambient pressure up to 180 GPa. This is in contrast with magnesium in which the hcp phase, which displays a c/a ratio of 1.62 at ambient conditions, transforms into bcc around 50 GPa.[11] The recent observation of a double hcp phase at high temperatures between 4 and 20 GPa (Ref. 22) suggests that the high-temperature range of stability of bcc Mg starts only at pressures larger than 20 GPa, in contrast to the calculated expectations.[23]

The reverse bcc-hcp Burgers mechanism, found with increasing pressure in Mg and increasing temperature in Be, involves the combination of a tensile deformation $e_{xx} - e_{yy}$, which lowers the hcp symmetry to orthorhombic $Cmcm$,[2] and antiparallel displacements of adjacent (001) layers by $\pm\frac{1}{12}[120]_{hcp}$, which yield the bcc structure.[4,6]

B. Calcium

At ambient conditions, Ca is fcc and transforms to bcc at 19.5 GPa.[16] With increasing pressure, Ca further transforms at 32 GPa to a simple cubic structure,[16] which remains stable in a wide pressure range up to 109 GPa.[12] Two additional phases have been recently disclosed[12] above 113 and 139 GPa, the structures of which remain to be determined. The fcc-bcc transition is also observed at ambient pressure at 721 K,[2] the transition temperature increasing to 823 K at 4 GPa.[2] From the specific form of the melting curve, that was determined up to 80 GPa,[24] it can be inferred that at high temperature the range of stability of the bcc phase is also limited below about 32 GPa at which the simple cubic phase takes place.
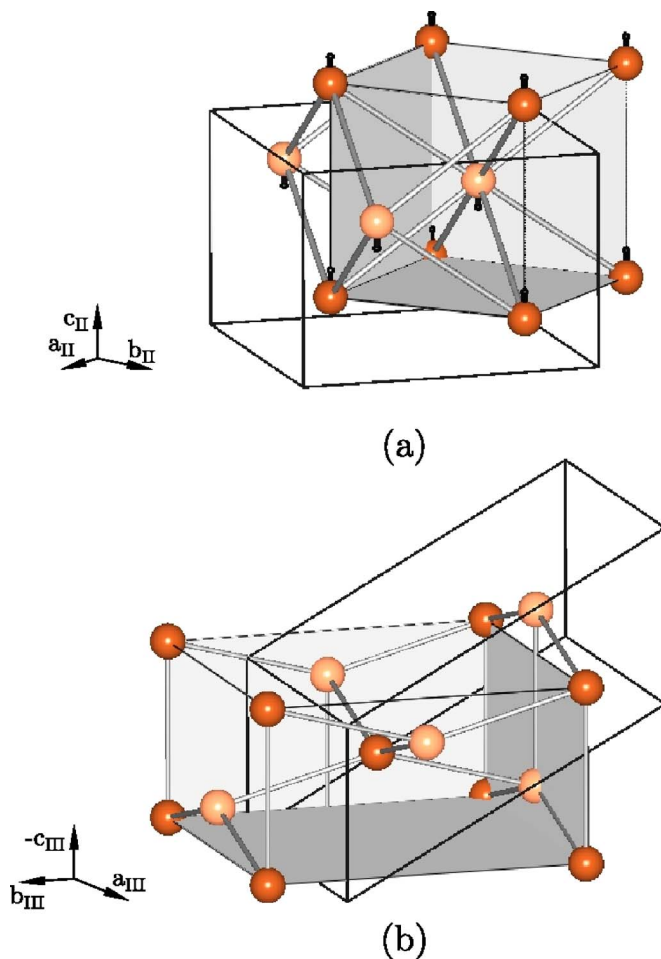
FIG. 3. (Color online) (a) Displacive mechanism associated with the Sr II→Sr III transition. The bcc structure of Sr II is transformed into the β-Sn-related structure of Sr III by antiparallel displacements of $\pm1/8\,[001]_{bcc}$ and a shear deformation lowering the $Cmcm$ symmetry of the common substructure (solid lines) to monoclinic $C2/m$. (b) β-Sn structure of Sr III represented by its conventional tetragonal unit cell (polyhedron) and the monoclinic $C2/m$ unit cell of the common substructure.

The fcc-bcc reverse Bain deformation mechanism taking place at 19.5 GPa involves a compression along the fourfold axis with the onset of the spontaneous shear strain $2e_{zz} - e_{xx} - e_{yy}$. For an arbitrary value of the strain the bcc $Im\bar{3}m$ symmetry reduces to tetragonal $I4/mmm$. For the specific ratio $c/a = \sqrt{2}$ of the lattice parameters, the tetragonal symmetry increases to fcc.[4,6] The mechanism transforming bcc Ca II into the simple cubic structure of Ca III is represented in Fig. 2. It consists of a decompression of the primitive bcc rhombohedron, associated with the spontaneous shear strains $e_{xz} = e_{yz} = e_{xy}$, which lowers the bcc symmetry to $R\bar{3}m$. A decrease of the rhombohedral angle from 109.471° to 90° gives rise to the simple cubic structure of Ca III.

C. Strontium

The fcc-bcc reverse Bain deformation mechanism takes place between Sr I and Sr II both under pressure, at 3.5 GPa
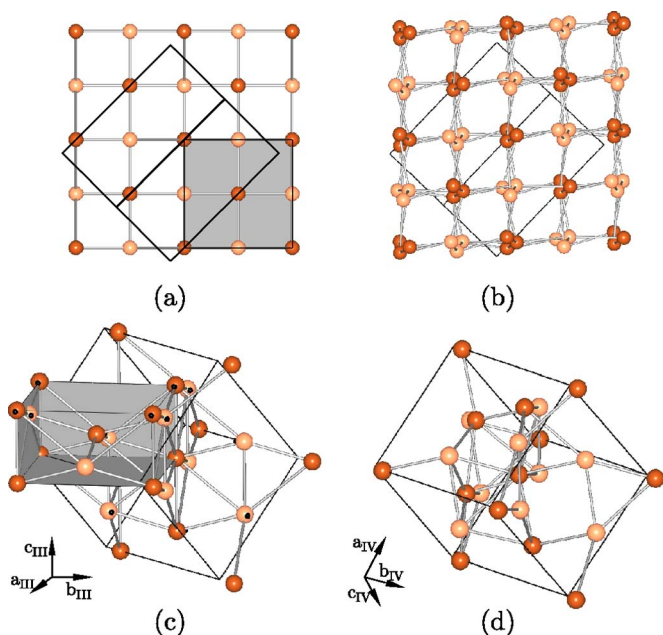
FIG. 4. (Color online) (a) Structure of Sr III, projected along [001]. The unit cell of the Sr III structure is shown as a polyhedron, while the unit cell of the Sr IV structure is represented by solid lines. (b) Structure of Sr IV, projected along [10$\bar{1}$]. (c) Relationship between the unit cells of Sr III and Sr IV shown in (d). The displacements associated with the Sr III→Sr IV phase transition are indicated by the small arrows. The origin of the transformed unit cell is shifted to $p=(0,1/8,0)$.

at room temperature, and with increasing temperature at 830 K at ambient pressure, the bcc phase occupying a wide region of the phase diagram below the melt.[1,2] At 25 GPa, the Sr III phase arises, which has the β-tin structure,[17] followed by the recently solved monoclinic Sr IV structure[18] at 37.7 GPa. The 36–37.7 GPa interval is occupied by a still undetermined "minority S" phase[13,18] that first appears as a smooth additional phase at the Sr II-Sr III transition and remains stable into the stability fields of Sr III, Sr IV, and Sr V, before transforming at 57 GPa into another additional phase that persists up to at least 75 GPa. The host-guest structure of Sr V appears at 46.3 GPa.[13] It is formed by a
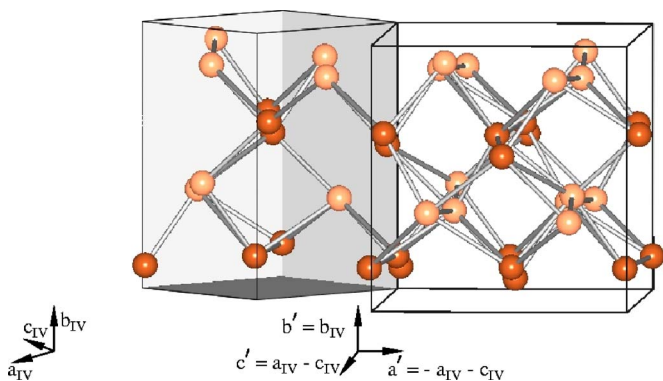
FIG. 5. (Color online) Relationship between the unit cells of the Sr IV phase (polyhedron) and the doubled "pseudo-orthorhombic" substructure (solid lines) common to Sr IV and Sr V.
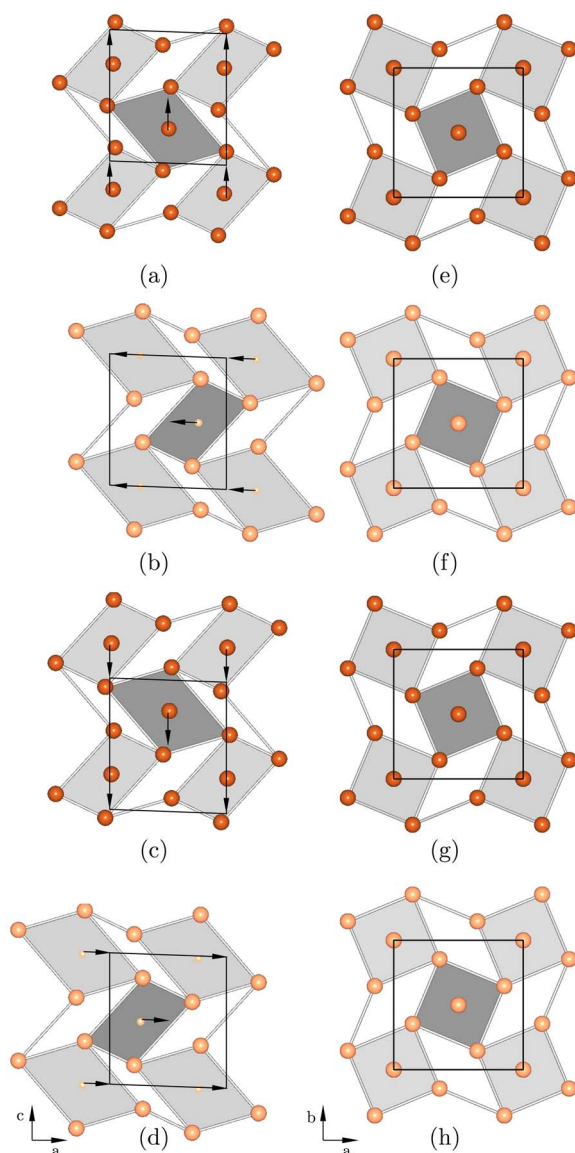
FIG. 6. (Color online) Structural relationship between the Sr IV and Sr V phases. [(a)–(d)] Layers 1–4 of Sr IV using the doubled "pseudo-orthorhombic" substructure of Sr IV which is shown in Fig. 5. [(e)–(h)] Corresponding layers of the Sr V structure. The unit cell of Sr V is doubled along c. The mechanism transforming Sr IV into Sr V is indicated by arrows.

host structure of symmetry $I4/mcm$ with $a=6.958$ Å and $c_H=3.959$ Å in which the Sr atoms occupy the Wyckoff position $8e$ (0.146 $x+1/2$ 0) and by a succession of two guest phases: A C-face-centered tetragonal phase with c_G =2.820 Å, which is stable up to 71 GPa and corresponds to the axial ratio $c_H/c_G=1.404$, followed by an undetermined guest structure which appears above 71 GPa.

Our proposed displacive mechanism for the Sr II-Sr III transition is shown in Fig. 3. The mechanism can be decomposed into two stages: Combined antiparallel displacements of the Sr atoms by $\pm\frac{1}{8}[001]_{bcc}$ and a shear deformation e_{xz} increasing the angle β from 90° to 118.39° lower the $Cmcm$ symmetry of the bcc substructure to monoclinic $C2/m$, with two atoms in the primitive unit cell. Figures 4(a) and 4(b)

and 4(c) and 4(d) show the close relationship between the Sr III and Sr IV structures and the set of displacements transforming the β-tin-type structure of Sr III into the monoclinic *Ia* structure of Sr IV [Fig. 4(d)]. The smallness of the calculated displacements is consistent with the almost continuous character reported for the Sr III-Sr IV transition[17] and with the group-subgroup relationship existing between the space groups of the two structures (see Sec. III).

The Sr IV structure is unique to Sr and its complexity has long resisted all attempts at solution. Its neighboring to the host-guest structure of Sr V is reminiscent of the complex Rb III structure which is adjacent to the host-guest structure of Rb IV.[25,26] This similarity is not fortuitous since, as shown in Fig. 5, a simple doubling of the Sr IV unit cell leads to a pseudo-orthorhombic conventional unit cell with $\mathbf{a}'=-\mathbf{a}-\mathbf{c}$, $\mathbf{b}'=\mathbf{b}$, and $\mathbf{c}'=\mathbf{a}-\mathbf{c}$ having 24 atoms and corresponding to the same orthorhombic $C222_1$ symmetry as Rb III. Moreover, the doubled unit cell coincides with the maximal substructure common to the Sr IV and Sr V structures, a property which allows understanding of the Sr IV-Sr V transition mechanism. Figure 6 shows the structural relationship between the two structures using the four-layer stacking of the pseudo-orthorhombic substructure. Figures 6(a)–6(d) indicate the alternate antiparallel displacements by $\pm1/4a$ and $\pm1/4c$ occurring in each layer, which yield the two-layer stacking forming the Sr V structure [Figs. 6(e)–6(h)]. An additional small shear deformation (e_{xz}) is required in order to transform the channels containing the guest atoms into regular square tubes. Note that in the Sr IV structure, the atoms forming the guest structure in Sr V are located above (layers 1 and 3) and below (layers 2 and 4) the planes, which are expanded by the atoms forming the host structure in Sr V. Figure 7 shows, respectively, a projection of the Sr V structure along [001] [Fig. 7(a)] and a perspective view of the structure [Fig. 7(b)].

D. Barium

bcc Ba I occupies the lower-pressure region of the phase diagram, transforming at 5.5 GPa to hcp Ba II,[1,2] which shows a strong pressure dependent c/a axial ratio, falling from about 1.58 at 7 GPa down to 1.50 (Refs. 14 and 27) at 12.6 GPa, before the transition to Ba IV. The self-hosting structure of Ba IV has a similar $I4/mcm$ host structure to Sr V with $a=8.4207$ Å and $c_H=4.7669$ Å, but different monoclinic (IVa), orthorhombic (IVb), and other (IVc, etc.) guest structures arising successively with increasing pressure.[19] The axial ratio $c_H/c_G=1.397$ for Ba IVa is slightly smaller than for Sr V and decreases with pressure to 1.3785 for Ba IVb.[19] hcp Ba V takes place at 45 GPa with an almost constant c/a ratio of 1.575.[14] The existence of the fcc Ba III structure reported below the melt, between 8 and 12 GPa,[27] has to be confirmed.

Our proposed structural mechanisms for the full sequence of high-pressure transitions taking place in barium are shown in Figs. 8 and 9. The $Cmcm$ substructure involved in the Ba I-Ba II Burgers mechanism [Figs. 8(a) and 8(b)] is transformed to an intermediate monoclinic substructure, shown in Fig. 8(c), by the shear deformation e_{yz}, which reduces the
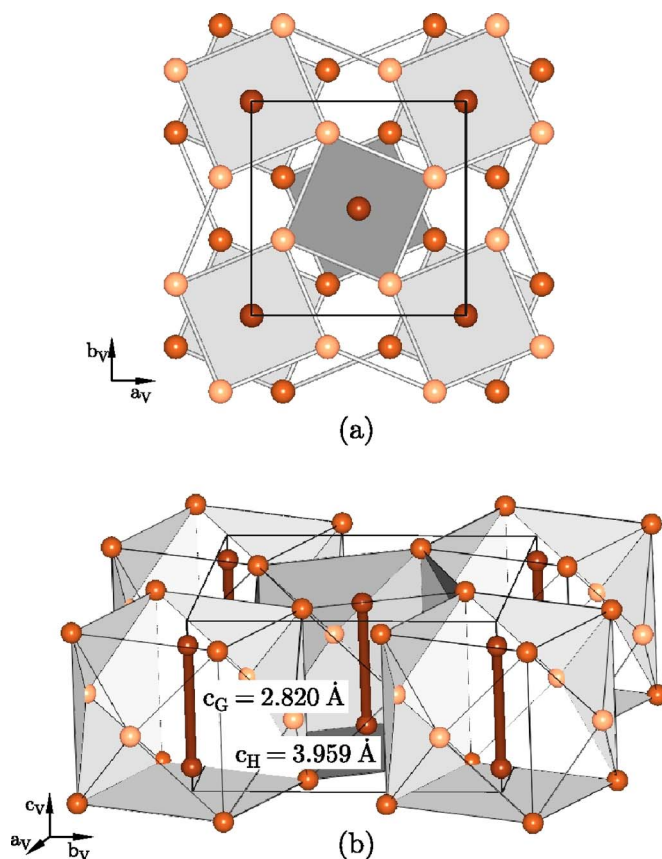
FIG. 7. (Color online) (a) Host-guest structure of Sr V, projected along [001]. (b) Perspective view of the Sr V structure showing the channels formed by the host structure as polyhedra. The guest atoms are located in the channels but can be disordered along the c axis. The ratio between the two c lattice vectors is incommensurate.

angle α from 90° to 81.17°. Antiparallel displacements of adjacent (001) hcp layers by $\pm\frac{1}{12}[\bar{1}10]_{hcp}$ transform the preceding substructure into an intermediate tetragonal substructure of symmetry $I4/mmm$, shown in Fig. 8(d), which becomes the Ba IV host-guest structure represented by the mechanism shown in Fig. 9. This rather complex mechanism involving two intermediate virtual substructures allows us to correlate the onset of the Ba IV structure for a c/a ratio in Ba II close to 1.5 and to the number of atoms contained in the host (10.78) and guest (7.76) unit cells. The unit cell of the tetragonal $I4/mmm$ intermediate substructure, corresponding to a commensurate Ba IV unit cell with ten atoms, has lattice constants of $a=3.776$ Å and $c=4.396$ Å intermediate between 4.7369 Å (host structure) and 3.4117 Å (guest structure), which in the monoclinic setting corresponds to a c/a axial ratio of 1.52. This is why the Ba II-Ba IV transition starts for c/a close to 1.5. The incommensurability of Ba IV is caused by an increase of the interlayer distances in the host lattice from $\frac{1}{2}$(4.396 Å) to $\frac{1}{2}$(4.7369 Å) and by a correlated decrease of the interatomic distances in the guest chains from 4.396 to 3.4117 Å. The Ba IV-Ba V transition mechanism implies the reverse path Ba IV-$I4/mmm-C2/m$-Ba V shown in Figs. 8(d)–8(f).
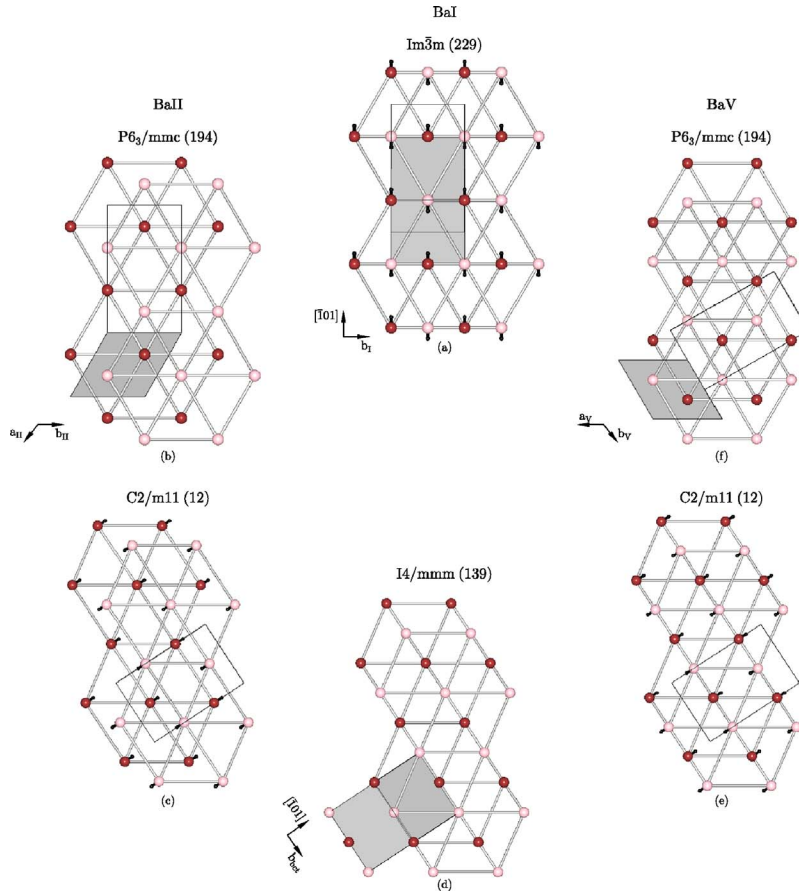
FIG. 8. (Color online) Burgers mechanism associated with the Ba I→Ba II→Ba IV→Ba V phase transitions. (a) The bcc structure of Ba I projected along [101] is transformed into the hcp structure of Ba II by antiparallel displacements of adjacent (101) layers by $\pm\frac{1}{12}[\bar{1}01]_{bcc}$ [arrows in (a)] and a tensile deformation (see text). (b) hcp structure of Ba II. (c) Monoclinic intermediate structure obtained by a shear deformation of the orthorhombic substructure of Ba II. Antiparallel displacements of adjacent (001) layers by $\pm\frac{1}{12}[\bar{1}10]_{hcp}$ transform the monoclinic substructure into a tetragonal substructure with symmetry $I4/mmm$ shown in (d). The $I4/mmm$ substructure is transformed into Ba IV by the mechanism shown in Fig. 9. (e) Further antiparallel displacements by $\pm\frac{1}{12}[10\bar{1}]_{bct}$ combined with a shear deformation yield the hexagonal close-packed structure of Ba V shown in (f). The conventional unit cells are shown as polyhedra, whereas the unit cells of the common substructure are represented by solid lines in (a)–(f).

III. SYMMETRY ANALYSIS AND DISCUSSION

Table I summarizes the connections between the different structures considered in the proposed transition mechanisms and the corresponding symmetry-breaking order parameters and macroscopic strains resulting from a Landau symmetry analysis. From Table I, one can deduce the symmetry relationships between the different high-pressure phases of the alkaline-earth metals, which are shown in Fig. 10. With the exception of the Sr III-Sr IV transition, all transitions in the group II possess a reconstructive character, i.e., they occur between group-subgroup unrelated structures, and therefore proceed via intermediate common substructures,[4] which are indicated by dotted rectangles in Fig. 10.

The thermodynamic paths relating the different structures in Fig. 10 show that the bcc phase can be taken as the parent structure for all the high-pressure alkaline-earth structures. Two main mechanisms are involved in the transitions. Burgers mechanism describes explicitly the Be II-Be I, Mg I-Mg II, and Ba I-Ba II transitions and is implicitly activated in the formation of the β-tin-type structure of Sr III from Sr II via the $Cmcm$ and $C2/m$ intermediate substructures (Fig. 3) corresponding to the bcc-hcp path. In the same way, the reverse Bain deformation mechanism describes explicitly the Ca I-Ca II and Sr I-Sr II transitions and is implicitly activated in the formation of the host-guest Ba IV structure, via the intermediate $I4/mmm$ substructure (Fig. 9) corresponding to the bcc-fcc Bain path. Moreover, from Table I and Fig. 10, one can see that the monoclinic Sr IV structure and the host

$I4/mcm$ structure of Sr V can be deduced from the Sr III structure by critical instabilities located on the W line $(\pi/a, \pi/a, k_z)$ of the body-centered-tetragonal (bct) Brillouin zone,[28] which coincides with the D line of the bcc Brillouin zone on which the N_4^- instability associated with Burgers mechanism is located. Analogously, the instability giving rise to the host Ba IV structure from the $I4/mmm$ intermediate Bain structure is located on the Θ surface (k_x, k_x, k_z) of the bct Brillouin zone coinciding with the bcc N surface which contains the N point. Thus, the Sr V host-guest structure appears as resulting from an incomplete Burgers mechanism in a material where the Bain deformation has been achieved at lower pressure. Conversely, the Ba IV host-guest structure results from an underlying Bain deformation, which occurs between two hcp structures reflecting the realization of Burgers mechanism.

The simple cubic Ca III structure appears at first glance as escaping from the preceding unifying scheme. However, it can also be interpreted as an intermediate stage toward the formation of an hcp structure, i.e., as an indirect attempt to realize Burgers mechanism. To make this point clear, one has to consider the monoclinic structure of symmetry $C2/m$, which represents, as shown in Fig. 11, the common substructure to the three cubic structures of Ca I, Ca II, and Ca III and to the rhombohedral $R\bar{3}m$ structure, assumed as an intermediate path for the Ca II-Ca III transition. Figure 12 shows that starting from any of the three cubic structures, one gets periodically the hcp structure for successive shifts of the Ca atoms along the **b**-monoclinic direction (coinciding with
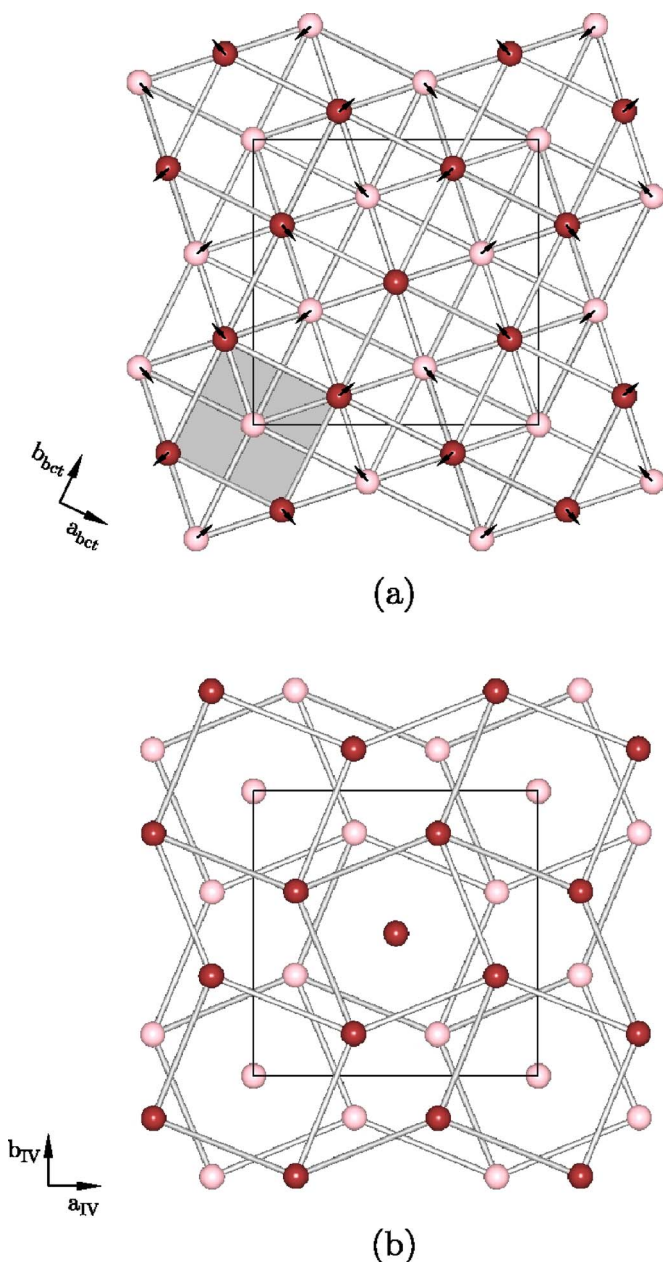
FIG. 9. (Color online) Displacive mechanism associated with the $I4/mmm \rightarrow$ Ba IV transition. The unit cell of the $I4/mmm$ structure projected along [001] is shown as a polyhedron in (a). The atomic displacements are indicated by arrows of the real magnitude. (b) Tetragonal host-guest structure of Ba IV projected along [001].

$[\bar{1}\,\bar{1}2]_{\text{fcc}}$, $[\bar{1}01]_{\text{bcc}}$, $[101]_{\text{sc}}$, and $[120]_{\text{hcp}}$) [Fig. 12(a)] combined with determined changes of the monoclinic angle α [Fig. 12(b)]. Thus, starting from the Ca III structure, corresponding to $\alpha=54.736°$, one gets the hcp structure for antiparallel displacements of $\pm\frac{1}{12}b$ and an increase of α to 90°. For general atomic shifts and $\alpha=90°$, for intermediate values of α without atomic displacements, or for general atomic shifts and noncritical values of α, one gets intermediate structures having either a $Cmcm$, a $I4/mmm$, or a $C2/m$ symmetry. It allows us to speculate that the still unknown structures of Ca IV and Ca V may display symmetries related

to the $Cmcm$-hcp or $I4/mmm$-hcp structural sequences.

In order to shed a different light on the respective role of Burgers and Bain mechanisms in the stabilization of alkaline-earth structures, let us refer to the evolution of the electronic configurations of the different elements on their pressure-induced polymorphism. In this respect, the current view is that except for beryllium and magnesium the crystallographic changes are strongly influenced by a nearly empty d band lying in close proximity to the s-p valence band, the d-band occupation increasing with atomic numbers and increasing pressure.[15] In Be, the d orbitals are lying at very high energies and remain essentially empty, the small c/a ratio in Be being ascribed to an increased p character of the valence electrons, which produces more anisotropic bonding properties and diminishes the close-packing ratio.[29] For Mg, the first empty d band is also far from the Fermi level and this explains why a high compression of 50 GPa is required for inducing the transition to the bcc structure attributed to an $sp \rightarrow d$ transition.[30] For the heavier elements, the increasing number of d electrons occupying the d band with increasing pressure is argued to be the essential driving force, but a different situation is assumed for Ca, Sr, and Ba. In Ca, the transfer of the s-p electrons into the d band is not achieved even at the high pressures corresponding to the Ca III phase, the Ca I $\rightarrow$ Ca II $\rightarrow$ Ca III transitions occurring for increasing critical values of the d-electron occupation number.[31] In Sr, the d band is essentially empty at ambient pressure, the Sr II $\rightarrow$ Sr III $\rightarrow$ Sr IV sequence being driven by increasing d occupancy.[32] By analogy with Ba IV,[33] the Sr V structure reflects dissociation in the spd hybridization with more d-like and more sp-like characters for the electronic structure of the host and guest atoms, respectively. The Ba V structure is suggested to be beyond the termination of the s-$p \rightarrow d$ transfer. The rapid decrease of the c/a ratio in Ba II is correlated to the increasing d occupancy, which favors short bond length and shorter c axis.

In order to relate the preceding description, derived from first-principles calculations, with our proposed structural mechanisms, it has to be viewed that the transfer of the s electrons into the p and d bands leads to a reduction of the charge density into the space between atoms and to a loss of intrinsic spherical symmetry of the atoms. The participation of p or d electrons in the bonding deforms the shape of the electronic shells and favors the formation of lower-symmetry structures due to the packing of nonspherical atoms. Although such geometrical representation oversimplifies the underlying quantum-mechanical considerations and complex hybridization process, it suggests the following link between the structural and electronic mechanisms described here.

The structural evolution under pressure in Be and Mg can be exclusively related to the $s \rightarrow p$ transfer, in agreement with the property of the first empty d band to be far above the Fermi level in both elements. Thus, the Mg I-Mg II transition occurs due to an increasing occupancy of the p band, which triggers the orthorhombic deformation involved in the reverse Burgers mechanism, inducing above 50 GPa a closer bcc than hcp packing of orthorhombically deformed atoms. At ambient temperature, the $s \rightarrow p$ transfer is insufficient in Be, even at 180 GPa, to destabilize the hcp packing, the more stable bcc Be I structure taking place only at higher

TABLE I. Structural changes and order parameters for the transitions in the alkaline-earth metals. The columns have the following meaning: (a) Space-group changes between the parent structure (left-hand side) and the final structure (right-hand side). (b) Basic vectors of the conventional unit cell of the final structure as function of the basic vectors of the conventional unit cell of the parent structure. (c) Ratio between the volumes of the conventional unit cells. (d) Irreducible representations (IR's) of the parent space group inducing the symmetry-breaking mechanism using the notations of Stokes and Hatch (Ref. 35), except for W_1 and $\Xi+\Delta$, where the notations of Zak *et al.* (Ref. 28) are used. $\Gamma_3^+(O)$ and $\Gamma_5^+(T)$ mean that the IR's refer to the orthorhombic and tetragonal Brillouin zones, respectively. (e) Dimension of the IR's and number of components of the order parameter. (f) Equilibrium relationship of the order-parameter components. (g) Secondary strains associated with the transitions. (h) Labeling of the phases of the alkaline-earth metals involved in the structural change. In columns (f) and (g), $e_1=e_{xx}-e_{yy}$, $e_2=2e_{zz}-e_{xx}-e_{yy}$, and $e_3=e_{xx}+e_{yy}+e_{zz}$.

(a)	(b)	(c)	(d)	(e)	(f)	(g)	(h)
$Im\bar{3}m\rightarrow$ $P6_3/mmc$	$\mathbf{b}$, $\frac{1}{2}(\mathbf{c}-\mathbf{a}-\mathbf{b})$, $\mathbf{a}+\mathbf{c}$	1	$N_4\left(\frac{\pi}{a},\frac{\pi}{a},0\right)$ $+\Gamma_5^+$	6 $+2$	$\eta_1\neq0$, $\eta_{2\rightarrow6}=0$, $e_1\neq0$, $e_{xy}=0$	e_{zz}	Ba I$\rightarrow$Ba II Be II$\rightarrow$Be I Mg II$\rightarrow$Mg I
$Im\bar{3}m\rightarrow Fm\bar{3}m$	$\mathbf{a}-\mathbf{b}$, $\mathbf{a}+\mathbf{b}$, $\mathbf{c}$	2	Γ_3^+	2	e_2, $e_{xx}=e_{yy}$	e_3	Ca II$\rightarrow$Ca I Sr II$\rightarrow$Sr I
$Im\bar{3}m\rightarrow Pm\bar{3}m$	$\frac{1}{2}(-\mathbf{a}+\mathbf{b}+\mathbf{c})$, $\frac{1}{2}(\mathbf{a}-\mathbf{b}+\mathbf{c})$, $\frac{1}{2}(\mathbf{a}+\mathbf{b}-\mathbf{c})$	$\frac{1}{2}$	Γ_5^+	3	$e_{xz}=e_{yz}=e_{xy}$		Ca II$\rightarrow$Ca III
$Im\bar{3}m\rightarrow$ $I4_1/amd$	$\mathbf{a}+\mathbf{b}$, $\mathbf{a}-\mathbf{b}+\mathbf{c}$, $-\mathbf{c}$	2	N_4^- $+\Gamma_3^+(O)$ $+\Gamma_5^+(T)$	6 $+1$ $+1$	$\eta_1\neq0$, $\eta_{2\rightarrow6}=0$ e_1 e_{xz}		Sr II$\rightarrow$Sr III
$I4_1/amd\rightarrow Ia$	$\frac{1}{2}(-\mathbf{a}+\mathbf{b}+3\mathbf{c})$, $\mathbf{a}+\mathbf{b}$, $\frac{1}{2}(-\mathbf{a}+\mathbf{b}-3\mathbf{c})$	3	$W_1\left(\frac{\pi}{a},\frac{\pi}{a},\frac{2\pi}{3c}\right)$	4	$\eta_1\neq0$, $\eta_{2\rightarrow4}=0$	e_{xz}, e_1	Sr III$\rightarrow$Sr IV
$I4/mcm\rightarrow Ia$	$\frac{1}{2}(\mathbf{a}+\mathbf{b})$, $2\mathbf{c}$, $\frac{1}{2}(\mathbf{a}-\mathbf{b})$	1	$P_5\left(\frac{\pi}{a},\frac{\pi}{a},\frac{\pi}{c}\right)$	4	$\eta_1\neq0$, $\eta_{2\rightarrow4}=0$	e_{xz}, e_1	Sr V$\rightarrow$Sr IV
$Im\bar{3}m\rightarrow$ $I4/mcm$	$2\mathbf{a}+\mathbf{b}$, $2\mathbf{b}-\mathbf{a}$, $\mathbf{c}$	5	Ξ $\Delta\left(\frac{4\pi}{5a},\frac{2\pi}{5a},\frac{2\pi}{a}\right)$	$+24$	$\eta_1=\eta_2\neq0$, $\eta_{3\rightarrow24}=0$	e_2	Ba I$\rightarrow$Ba IV

temperatures, where an increase of the Debye-Waller factor permits a closer bcc than hcp packing, due to the interpenetration of "softer" atomic shells.

In Sr and Ba, the combined structural and electronic descriptions clarify the competing mechanisms giving rise to the frustrated Sr V and Ba IV host-guest structures. In Sr, the tendency to form tetragonal structures is favored by increasing d occupancy with increasing pressure and results into the host structure of Sr V. It is balanced by the unachieved Burgers mechanism, which gives rise to Sr III and Sr IV and yields the guest Sr V structures. On the contrary, the host structure of Ba IV expresses a frustrated attempt to realize the Bain deformation, whereas the successive Ba IV guest structures, with orthorhombic and monoclinic symmetries, reflect the tendency to achieve the Burgers mechanism initiated with hcp Ba II and ending with hcp Ba V. The respective increase and decrease of the interlayer distances in the host and guest structures of Sr V and Ba IV, which yield the incommensurate character of the host-guest structures, can be related to the packing of differently deformed nonspherical atoms.

Ca is at the borderline between the lighter and heavier alkaline-earth mechanisms. The first-principles calculations by Ahuja *et al.*[31] provide convincing arguments for relating the Ca II-Ca III strongly reconstructive transition to the increased d occupancy of Ca. The structural mechanisms shown in Figs. 11 and 12 suggest that Ca IV and Ca V should confirm an evolution to structural configurations reflecting the realization of Burgers mechanism under the form of an intermediate orthorhombic or tetragonal structure (or a tetragonally based host-guest structure) for Ca IV, followed by an hcp structure.

IV. SUMMARY AND CONCLUSION

In summary, the different high-pressure structures observed in the elements of group II have been related by dis-
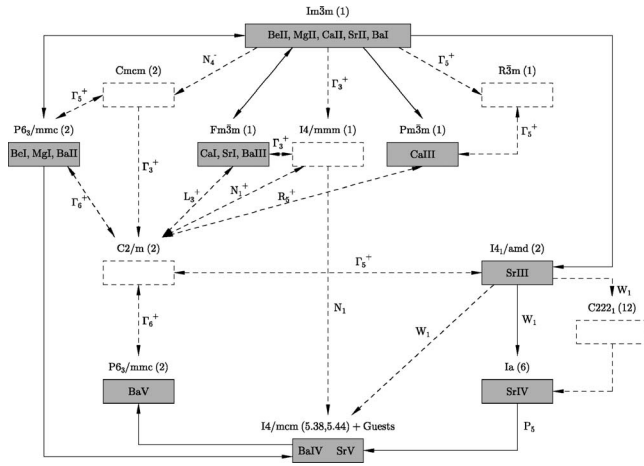
FIG. 10. Connections between the structures observed in alkaline-earth metals. The irreducible representations associated with the symmetry-breaking mechanisms are indicated by simple or double arrows relating the structures. The notation of Stokes and Hatch is used (Ref. 35), except for the W_1, and N_1 irreducible representations, which correspond to the notation of Zak *et al.* (Ref. 28). The intermediate unobserved structures assumed in our mechanisms are indicated by white boxes.

placive atomic mechanisms. Except for the Sr III→Sr IV transition, all structural mechanisms display a reconstructive character, which requires going through unobserved intermediate structures. The analysis of the proposed mechanisms shows that all the high-pressure phases of alkaline-earth metals can be interpreted as resulting from the full or incomplete realization of the Burgers and Bain deformation mechanisms. The competition between these two mechanisms in the same element explains, at the structural level, the formation of the host-guest Sr V and Ba IV structures, and may possibly influence the high-pressure structures of calcium, above the region of stability of the Ca III structure. At the electronic level, the host-guest structures express the competition between the increasing occupation of the *d* bands with increasing pressure and the remaining influence of the hybridized *s*-*p* electrons. Therefore, the formation of host-guest structures appears as the best compromise for realizing close-packed structures at high pressure when competing, structural and electronic, mechanisms are involved. This interpretation holds not only for the alkaline-earths metals but also for alkali metals,[34] where the formation of host-guest structures in K and Rb is due, on the one hand, to the
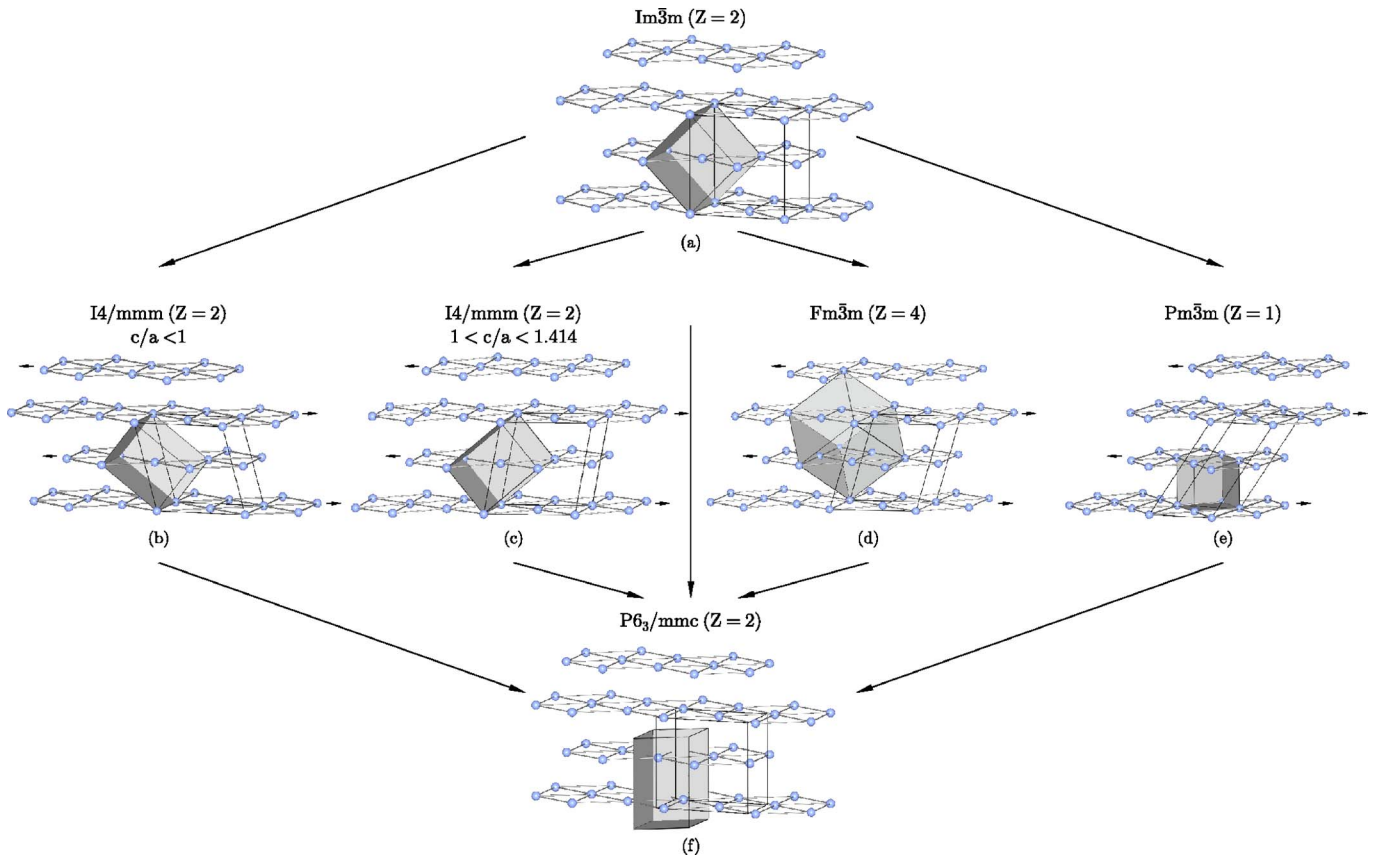
FIG. 11. (Color online) Structural mechanisms for the reconstructive phase transitions in group II elements via a common substructure: (1) bcc→bct [(a)→(b) and (a)→(c)], (2) bcc→fcc [(a)→(d)], (3) bcc→simple cubic [(a)→(e)], (4) bcc→hcp [(a)→(f)], (5) bct →hcp [(b)→(f) and (c)→(f)], (6) fcc→hcp [(d)→(f)], and (8) simple cubic→hcp [(e)→(f)]. The conventional cubic (bcc, fcc, simple cubic), tetragonal (bct), and hexagonal (hcp) unit cells are represented by gray polyhedra in (a), (d), (e), (b), (c), and (f). The unit cells of the common $Cmcm$ [(a) and (f)] or $C2/m$ [(b)–(e)] substructures are shown by solid lines. The small arrows in (b), (c), (d), and (e) represent the shifting of the $(101)_{bct}$ [(b) and (c)], $(112)_{fcc}$ [(d)], and $(121)_{sc}$ [(e)] layers by $\pm\frac{1}{12}[\bar{1}01]_{bct}$, $\pm\frac{1}{24}[\bar{1}\bar{1}2]_{fcc}$, and $\pm\frac{1}{12}[101]_{sc}$, respectively, associated with the (bct, fcc, sc)→hcp phase transitions.

electronic frustration related to the increasing d occupancy and also to the onset of structures (as the *Cmca* structure of Rb VI and Cs V) resulting from mechanisms different from the bcc-fcc Bain deformation, which dominates at lower pressure.

Alkaline-earth metals are usually assumed to present strong similarities with alkali metals because the elements of the two groups display large volumes and compressibilities, and nearby empty d bands which influence their structural evolution under pressure. However, there is an essential property differentiating their phase diagrams: The Bain deformation occurs uniformly for the lower-pressure transitions in alkali metals, and an hcp phase, reflecting the influence of Burgers mechanism, appears only with the highest-pressure phase of Cs. In contrast, the present study shows that there is a complex crossover between the two mechanisms in the high-pressure polymorphism of alkaline-earth metals.

In conclusion, a number of key results, that can stimulate further studies, can be inferred from our theoretical description of the structural mechanisms in alkaline-earth metals.

At the Sr III→Sr IV transition between 36 and 37.7 GPa, Bovornratanaraks *et al.*[18] observed that the (200) and (020) reflections continue to overlap as a singlet which cannot be accounted for by the monoclinic structure of Sr IV. The nonsplitting of these reflections is consistent with the higher orthorhombic symmetry $C222_1$ of the intermediate structure assumed for the Sr III→Sr IV transition mechanism. The existence of a narrow interval of stability for this structure, similar to the narrow interval of stability found for Cs III,[26] would provide an additional example of complex orthorhombic modulated structure, with 24 atoms in the conventional C-centered unit cell.

Our description of the host-guest structures as resulting from a competition of two structural mechanisms may help clarify the relationship between the guest structures and the order in their sequences in Ba IV and Sr V. Thus, the monoclinic (IVa), orthorhombic (IVb), and further barium guest structures (IVc, IVd, etc.) should represent successive intermediate stages for achieving Burgers mechanism on the way to the Ba V hcp structure. Analogously, the tetragonal C-centered and undetermined guest structures of Sr V should be viewed as unachieved steps in realizing an hcp structure. The disorder observed for the guest structures in both elements can also be related to the frustration induced by the competition between Burgers and Bain mechanisms.

The prediction of the highest-pressure hcp structure in calcium with an intermediate phase realizing one of the possible substructure common to the Ca III and hcp structures can be checked by the determination of the Ca IV and Ca V structures.

The intermediate structures assumed in the mechanisms relating the alkaline-earth structures (Fig. 10) should not be
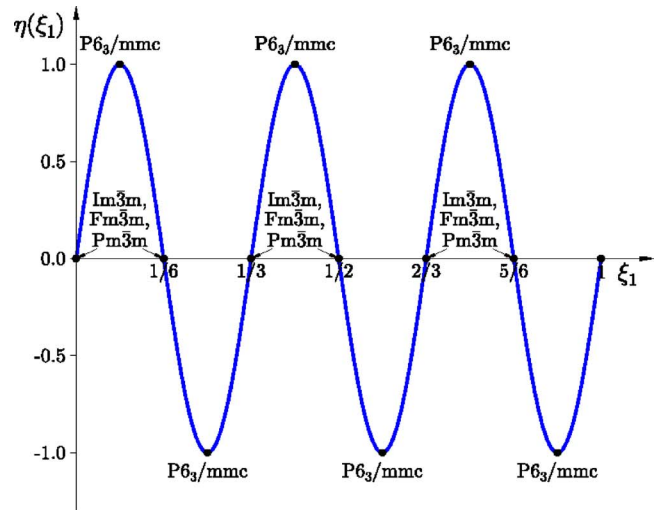
(a)
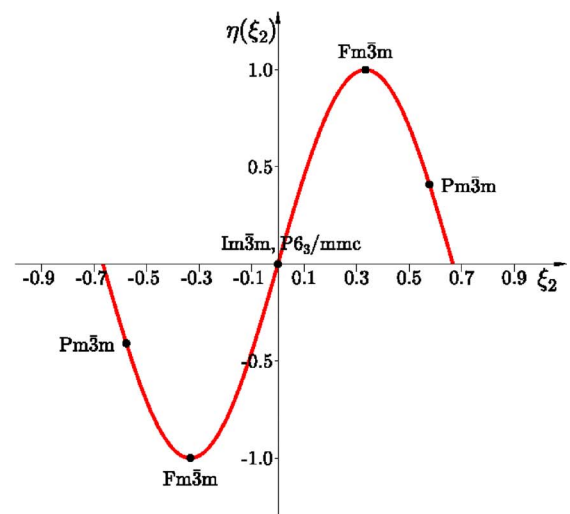
(b)

FIG. 12. (Color online) Sinusoidal dependence of the order parameter $\eta(\xi_1, \xi_2)$ given as $\eta(\xi_1, \xi_2) = \sin(6\pi\xi_1) + \sin(3/2\pi\xi_2)$. (a) Periodic dependence of the order parameter $\eta(\xi_1)$ as function of the displacements ξ_1 along the orthorhombic and/or monoclinic b axis of the common substructure corresponding to the $[\bar{1}01]_{bcc}$, $[\bar{1}\bar{1}2]_{fcc}$, $[101]_{sc}$, and $[120]_{hcp}$ directions. (b) Periodic dependence of the order parameter $\eta(\xi_2)$ for $\xi_1 = 0, \pm\frac{1}{6}, \pm\frac{1}{3}, \pm\frac{1}{2}, \pm\frac{2}{3}, \pm\frac{5}{6}, \pm 1$. ξ_2 represents $\cos\alpha$ of the common substructure.

observed due to the strongly reconstructive character of the transitions, but they can be tested as representing the minimal energy paths in total-energy calculations.

*Electronic address: hanne@min.uni-kiel.de

[1] D. A. Young, *Phase Diagrams of the Elements* (University of California Press, Berkeley, 1991).

[2] E. Yu Tonkov and E. G. Ponyatovsky, *Phase Transformations of Elements Under High Pressure* (CRC, Boca Raton, 2005).

[3] W. G. Burgers, Physica (Amsterdam) **1**, 561 (1934).

[4] P. Tolédano and V. Dmitriev, *Reconstructive Phase Transitions* (World Scientific, Singapore, 1996).

[5] V. P. Dmitriev, S. B. Rochal, Yu. M. Gufan, and P. Tolédano, Phys. Rev. Lett. **60**, 1958 (1988).

[6] V. P. Dmitriev, Yu. M. Gufan, and P. Tolédano, Phys. Rev. B **44**, 7248 (1991).

[7] E. C. Bain, Trans. AIME **70**, 25 (1924).

[8] B. Mettout, V. P. Dmitriev, M. Ben Jaber, and P. Tolédano, Phys. Rev. B **48**, 6908 (1993).

[9] V. P. Dmitriev, A. Yu. Kuznetsov, D. Machon, H.-P. Weber, and P. Tolédano, Europhys. Lett. **61**, 783 (2003).

[10] W. J. Evans, M. J. Lipp, H. Cynn, C. S. Yoo, M. Somayazulu, D. Hausermann, G. Shen, and V. Prakapenka, Phys. Rev. B **72**, 094113 (2005).

[11] H. Olijnyk and W. B. Holzapfel, Phys. Rev. B **31**, 4682 (1985).

[12] T. Yabuuchi, Y. Nakamoto, K. Shimizu, and T. Kikegawa, J. Phys. Soc. Jpn. **74**, 2391 (2005).

[13] M. I. McMahon, T. Bovornratanaraks, D. R. Allan, S. A. Belmonte, and R. J. Nelmes, Phys. Rev. B **61**, 3135 (2000).

[14] Takemura Kenichi, Phys. Rev. B **50**, 16238 (1994).

[15] H. L. Skriver, Phys. Rev. Lett. **49**, 1768 (1982).

[16] H. Olijnyk and W. B. Holzapfel, Phys. Lett. **100A**, 191 (1984).

[17] D. R. Allan, R. J. Nelmes, M. I. McMahon, S. A. Belmonte, and T. Bovornratanaraks, Rev. High Pressure Sci. Technol. **7**, 236 (1998).

[18] T. Bovornratanaraks, D. R. Allan, S. A. Belmonte, M. I. Mc-Mahon, and R. J. Nelmes, Phys. Rev. B **73**, 144112 (2006).

[19] R. J. Nelmes, D. R. Allan, M. I. McMahon, and S. A. Belmonte, Phys. Rev. Lett. **83**, 4081 (1999).

[20] J. Donohue, *The Structure of the Elements* (Robert E. Krieger, Malabar, 1982).

[21] J. Elmsley, *The Elements* (Oxford University Press, London, 1998).

[22] D. Errandonea, Y. Meng, D. Häusermann, and T. Uchida, J. Phys.: Condens. Matter **15**, 1277 (2003).

[23] J. A. Moriarty and J. D. Althoff, Phys. Rev. B **51**, 5609 (1995).

[24] D. Errandonea, R. Boehler, and M. Ross, Phys. Rev. B **65**, 012108 (2001).

[25] R. J. Nelmes, M. I. McMahon, J. S. Loveday, and S. Rekhi, Phys. Rev. Lett. **88**, 155503 (2002).

[26] M. I. McMahon, S. Rekhi, and R. J. Nelmes, Phys. Rev. Lett. **87**, 055501 (2001).

[27] M. Winzenick and W. B. Holzapfel, Phys. Rev. B **55**, 101 (1997).

[28] J. Zak, A. Cacher, H. Glück, and Y. Gur, *Irreducible Representations of Space Groups* (Benjamin, New York, 1969).

[29] M. Y. Chou, Pui K. Lam, and M. L. Cohen, Phys. Rev. B **28**, 4179 (1983).

[30] J. A. Moriarty and A. K. McMahan, Phys. Rev. Lett. **48**, 809 (1982).

[31] R. Ahuja, O. Eriksson, J. M. Wills, and B. Johansson, Phys. Rev. Lett. **75**, 3473 (1995).

[32] R. Ahuja, B. Johansson, and O. Eriksson, Phys. Rev. B **58**, 8152 (1998).

[33] S. K. Reed and G. J. Ackland, Phys. Rev. Lett. **84**, 5580 (2000).

[34] H. Katzke and P. Tolédano, Phys. Rev. B **71**, 184101 (2005).

[35] H. T. Stokes and D. M. Hatch, *Isotropy Subgroups of the 230 Crystallographic Space Groups* (World Scientific, Singapore, 1988).